^{13}C and ^{15}N Isotope Effects for Conversion of L-Dihydroorotate to *N*-Carbamyl-L-aspartate Using Dihydroorotase from Hamster and *Bacillus caldolyticus*†

Mark A. Anderson,‡ W. Wallace Cleland,*,‡ Danny T. Huang,§ Camilla Chan,§ Maryam Shojaei,§ and Richard I. Christopherson§

Institute for Enzyme Research, Department of Biochemistry, University of Wisconsin—Madison, 1710 University Avenue, Madison, Wisconsin 53726, and School of Molecular and Microbial Biosciences, Maze Crescent, University of Sydney, Sydney, NSW 2006, Australia

Received February 28, 2006; Revised Manuscript Received April 18, 2006

ABSTRACT: In the pyrimidine biosynthetic pathway, *N*-carbamyl-L-aspartate (CA-asp) is converted to L-dihydroorotate (DHO) by dihydroorotase (DHOase). The mechanism of this important reaction was probed using primary and secondary ^{15}N and ^{13}C isotope effects on the ring opening of DHO using isotope ratio mass spectrometry (IRMS). The reaction was performed at three different temperatures (25, 37, and 45 °C for hamster DHOase; 37, 50, and 60 °C for *Bacillus caldolyticus*), and the product CA-asp was purified for analysis. The primary and secondary kinetic isotope effects for the ring opening of the DHO were determined from analysis of the N and C of the carbamyl group after hydrolysis. In addition, the β-carboxyl of the residual aspartate was liberated enzymatically by transamination to oxaloacetate with aspartate aminotransferase and then decarboxylation with oxaloacetate decarboxylase. The $^{13}C/^{12}C$ ratio from the released CO_2 was determined by IRMS, yielding a second primary isotope effect. The primary and secondary isotope effects for the reaction catalyzed by DHOase showed little variation between enzymes or temperatures, the primary ^{13}C and ^{15}N isotope effects being approximately 1% on average, while the secondary ^{13}C isotope effect is negligible or very slightly normal (>1.0000). These data indicate that the chemistry is at least partially rate-limiting while the secondary isotope effects suggest that the transition state may have lost some bending and torsional modes leading to a slight lessening of bond stiffness at the carbonyl carbon of the amide of CA-asp. The equilibrium isotope effects for DHO → CA-asp have also been measured (secondary $^{13}K_{eq} = 1.0028 \pm 0.0002$, primary $^{13}K_{eq} = 1.0053 \pm 0.0003$, primary $^{15}K_{eq} = 1.0027 \pm 0.0003$). Using these equilibrium isotope effects, the kinetic isotope effects for the physiological reaction (CA-asp → DHO) have been calculated. These values indicate that the carbon of the amide group is more stiffly bonded in DHO while the slightly lesser, but still normal, values of the primary kinetic isotope effect show that the chemistry remains at least partially rate-limiting for the physiological reaction. It appears that the ring opening and closing is the slow step of the reaction.

Dihydroorotase (DHOase;[1] E.C. 3.5.2.3) is a zinc metalloenzyme that catalyzes the reversible cyclization of *N*-carbamyl-L-aspartate (CA-asp) to L-dihydroorotate (DHO), the third step in de novo pyrimidine biosynthesis (Scheme 1). This enzyme has been rigorously studied [kinetics (*1*, *2*), pH profiles (*2*), inhibition studies (*3*−*6*), X-ray crystallography (*7*−*9*), etc.] for the last 25 years, and many facts about the protein structure and function are now known.

Scheme 1

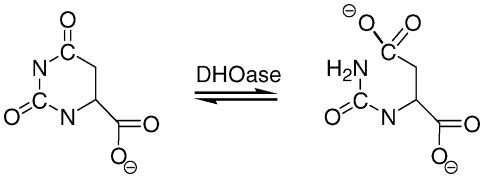

Amino acid sequence alignments have determined that DHOase belongs to the amidohydrolase superfamily of enzymes that also includes urease, phosphotriesterase, and adenosine deaminase (*10*). This superfamily is predicted to have a TIM barrel motif and a familiar pattern of four conserved histidine residues and one aspartate residue. One or two Zn ions are held firmly in the active site. This superfamily consists primarily of two distinct subsets. The first (which includes urease and phosphotriesterase) has a binuclear metal (Zn) center. The divalent metal centers are separated by 3.6 Å and ligated to the protein through

† Supported by research grants from the National Institutes of Health (GM18938) and the Australian National Health and Medical Research Council (253781).

* To whom correspondence should be addressed. E-mail: cleland@biochem.wisc.edu. Phone: (608) 262-1373. Fax: (608) 265-2904.

‡ Institute for Enzyme Research, University of Wisconsin.

§ School of Molecular and Microbial Biosciences, University of Sydney.

[1] Abbreviations: DHOase, dihydroorotase; hDHOase, recombinant dihydroorotase domain from hamster; BcDHOase, recombinant dihydroorotase from *Bacillus caldolyticus*; CA-asp, *N*-carbamyl-L-aspartate; DHO, L-dihydroorotate; IRMS, isotope ratio mass spectrometry.

10.1021/bi0604025 CCC: $33.50
Published on Web 05/19/2006

electrostatic interactions with the side chains of six amino acids. One Zn ion is more buried in the structure, ligated by two histidine residues and one aspartate residue and is termed the α metal center, M_α. The second Zn ion is much more solvent exposed, ligated by two histidine residues and is known as the β metal center, M_β (*11*). These metal centers are bridged by a solvent hydroxide and a carbamate functional group from the posttranslational modification of a lysine residue (*7*, *11*). The second subset of this superfamily (that includes adenosine deaminase) has a single five-coordinate Zn ion where the ligands are three conserved histidine residues, a single conserved aspartate, and a solvent H_2O molecule (*12*). The carboxylated lysine residue is absent in the second subset.

There are examples of a third and possibly fourth smaller subset in the amidohydrolase superfamily. In these cases members with a single divalent cation at the β site and some that require no metal ion at all have been discovered (*11*). However, neither type has been reported for a DHOase where only two crystal structures are available.

Phylogenetic analysis of amino acid sequences of DHOases shows two types (types I and II) that share a common ancestor with other amidohydrolases (*13*). Analysis of sequence alignments has shown that type I DHOases are older than type II (*13*). They are also larger at ∼45 kDa and contain one bound zinc atom at the active site (*13*). Examples of type I DHOases are the DHOase domain from trifunctional CAD of hamster and the enzymes from *Bacillus caldolyticus* and *Aquifex aeolicus*. A three-dimensional structure is available for the latter with a cysteine ligand that blocks the site for the inactive form (*2*, *13*, *14*). Type II DHOases are smaller (∼38 kDa) and contain two zinc atoms at the active site bridged by a carboxylated lysine residue, exemplified by the DHOase from *Escherichia coli* for which a three-dimensional structure has been determined (*7*, *15*).

In this study, the type I DHOases from hamster and the thermophilic bacterium *B. caldolyticus* were produced and purified, and the physiological reverse reaction of DHO → CA-asp was run at various temperatures. The product, CA-asp, was acid hydrolyzed to CO_2, NH_4Cl, and aspartic acid. These components were studied by IRMS, allowing two primary kinetic isotope effects and one secondary kinetic isotope effect to be calculated for this enzymatic conversion. The primary kinetic isotope effects indicate whether the chemistry of this enzymatic reaction is completely or at least partially rate-limiting while the secondary effects give information on the differences in bond orders between the ground and transition states. The equilibrium isotope effects were also determined. Experimentally determined equilibrium isotope effects and kinetic isotope effects were then used to calculate kinetic isotope effects for the physiological reaction of CA-asp → DHO.

MATERIALS AND METHODS

Enzyme Preparation. Recombinant hamster dihydroorotase (hDHOase) was overexpressed from *E. coli* K strain SØ1263/ pyrC$^-$ transformed with pCW25 containing the hamster DHOase domain with an extra 33 amino acid residues into the bridge region and purified as described previously (*16*). The purified enzyme was stored in 20 mM Hepes, pH 7.3, 10% (v/v) glycerol, 0.1 mM EDTA, and 1 mM DTT.

The pyrC gene from *B. caldolyticus* was PCR amplified from a plasmid, pSY188, with primers 5′-GTCCAC-CATGGGCGTATGGCTGAAAAATGGC-3′ and 5′-CAGC-CGGATCCTTACGCCCTTCCTTTCTCCCATAC-3′ containing *Nco*I and *Bam*HI restriction sites, respectively. The PCR product was cloned into the pET3c vector (Novagen) and subsequently transformed into *E. coli* BL21(DE3) cells. The cells were grown at 37 °C, harvested, and lysed in 20 mM K-Hepes, pH 7.5, and 0.15 mM PMSF and then centrifuged (39000*g*, 30 min, 4 °C). The cell lysate was fractionated with 2.5% (w/v) streptomycin sulfate and centrifuged (39000*g*, 4 °C, 20 min). The supernatant was incubated at 60 °C with shaking for 6 min, then immediately cooled on ice, and centrifuged (39000*g*, 4 °C, 20 min). The supernatant was then loaded onto a PorosHQ column in 20 mM K-Hepes, pH 7.5, and eluted with a 0−1 M NaCl gradient. BcDHOase eluted at ∼300 mM NaCl. A second passage through the PorosHQ column yielded protein with >95% purity.

Dihydroorotase Assay. The reaction was assayed in the degradative direction (DHO → CA-asp). For kinetic isotope analysis, the reaction mixture contained 50 mM K-Hepes, pH 8.0, 5% (v/v) glycerol, and 20 mM DHO. The pH of the buffer was adjusted to 8.0 at the appropriate temperatures of the reaction. Three different temperatures (25, 37, and 45 °C for hDHOase; 37, 50, and 60 °C for BcDHOase) were assayed in duplicate. (For each enzyme, less than optimal temperatures were used.) The reaction was initiated by addition of hDHOase (1−3 mg) or BcDHOase (0.2−0.8 mg) to give a final volume for the reaction of 5.0 mL. The partial reaction (∼35−50% conversion) and complete reaction were determined by monitoring the decrease in absorbance at 230 nm, ϵ(DHO) = 1170 M^{-1} cm^{-1}. The times to stop the reaction for partial and complete conversion were determined by performing a small-scale reaction. An aliquot of 1 or 1.3 mL of 0.5 M HCl was added to the hDHOase or BcDHOase mixture, respectively, to stop the reaction, which was cooled on ice. Addition of this amount of HCl brought the pH down to 2.8−3.5, sufficient to denature the protein and prevent the forward reaction (CA-asp → DHO). Addition of NaOH to pH 7.3 did not reactivate the enzyme. A 1 in 20 dilution of the reaction mixture in water was used to determine the absorbance at 230 nm. A zero time sample contained the same components as the reaction mixture except that HCl was added before the enzyme.

Purification of CA-asp. A Partisil 10 SAX column (250 × 4.60 mm) was used to separate CA-asp from DHO and other reaction mixture components. An aliquot of 150 μL of 1 M NaOH was added to each sample just prior to loading to bring the pH to ∼3.8−4.2 to ensure proper binding of CA-asp. Each reaction mixture was purified in three runs. The column was equilibrated in 7 mM potassium phosphate buffer, pH 5.7 (buffer A), and eluted with 0.25 M potassium phosphate buffer, pH 5.7, and 0.7 M KCl (buffer B). The separation was performed in the following steps: 0% B, 2 min; 0−100% B, 20 min; 100% B, 5 min; 100−0% B, 1 min at a flow rate of 1.5 mL/min. The column was reequilibrated with buffer A for 7 min prior to each sample injection. Fractions corresponding to CA-asp were pooled and lyophilized.

Nomenclature. The nomenclature used for describing isotope effects is that of Northrop (*17*). Isotope effects are

designated with a leading superscript corresponding to the isotope; thus $^{13}(V/K)$ and $^{15}(V/K)$ indicate the kinetic isotope effect for carbon and nitrogen, respectively, while $^{13}K_{eq}$ and $^{15}K_{eq}$ indicate equilibrium isotope effects. All isotope effects are the ratio of the parameter for the light atom to that of the heavy one.

Kinetic Isotope Effects for a Simple System. For a reaction that involves a one step process with no side or competing reactions, determining primary kinetic isotope effects in systems where a C−N bond is broken is very straightforward by the internal competition method. Changes in mass ratios of a substrate or product are followed as the reaction proceeds, the method of choice when using substrates with natural abundance of ^{13}C (1.1%) and ^{15}N (0.37%). This methodology along with the use of an IRMS allows for greater accuracy and precision than other systems. When a C−N bond is broken in the rate-limiting step of the reaction, the C and N atoms are isolated as CO_2 and N_2, respectively. No labeled syntheses are necessary, and changes in the mass ratios in the compound will be sufficient to determine the isotope effect. The reaction is run from 10% to 70% completion, and the amount of initial substrate that reacts, the fraction of reaction f, is determined accurately by UV−vis spectrophotometry (in these experiments). Each gas sample was analyzed individually by IRMS to determine its isotopic ratio compared to a known standard to give a δ value defined as

$$\delta = 1000\left[\left(\frac{^{15}N_{sample}/^{14}N_{sample}}{^{15}N_{standard}/^{14}N_{standard}}\right) - 1\right] \quad (1)$$

To determine the isotope effect, the samples were converted to an R value defined as

$$R = (\delta_{sample}/1000) + 1 \quad (2)$$

R values for the reaction product, R_P, and residual substrate, R_S, were used in the following equations to arrive at the isotope effect:

$$IE_{prod} = \frac{\ln(1-f)}{\ln[(1-f)(R_P/R_O)]} \quad (3)$$

$$IE_{sub} = \frac{\ln(1-f)}{\ln[(1-f)(R_S/R_O)]} \quad (4)$$

In these equations, R_O is the isotopic ratio of the starting material and f is the fraction of reaction.

Equilibrium Isotope Effects. The equilibrium isotope effect is the ratio of the equilibrium constant for the light isotope to that for the heavy isotope. Using N as an example

$$K_{eq}IE = K_{eq-14}/K_{eq-15} \quad (5)$$

Considering the reaction from DHO → CA-asp, $^{15}K_{eq}$ is equal to mass ratios of residual DHO and CA-asp formed. The reaction of DHO to CA-asp catalyzed by hDHOase was allowed to proceed at pH 6.0 and 25 °C, 10 times longer than necessary to reach equilibrium, yielding a product ratio of 35/65 CA-asp to DHO. DHO and CA-asp were acid hydrolyzed, the products were treated as shown in Scheme 2, and the mass ratios were determined as described above.

Scheme 2: Enzymatic Reaction of Dihydroorotate and Decomposition of CA-asp and Aspartic Acid for Isotope Effect Analysis

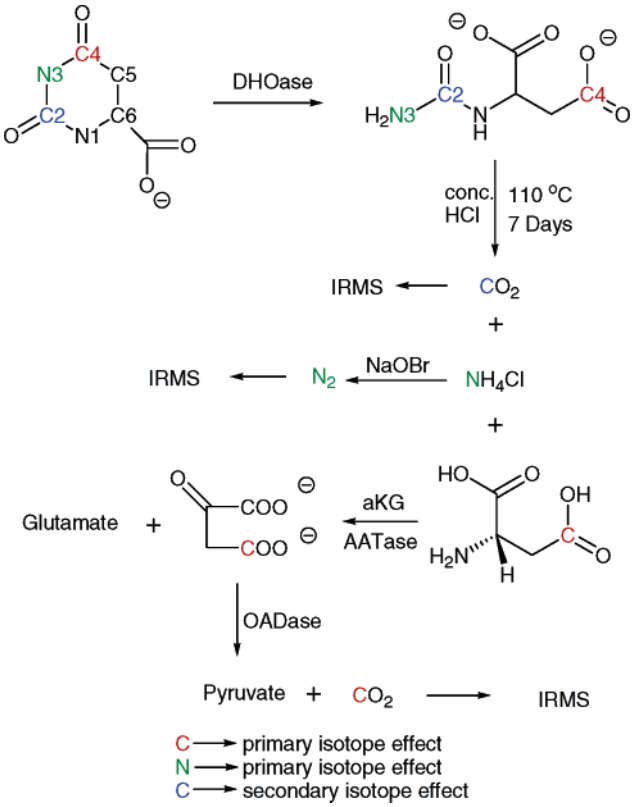

Calculation of Kinetic Isotope Effects for the Physiological Reaction of CA-asp to DHO Catalyzed by hDHOase. Primary and secondary isotope effects, for both ^{15}N and ^{13}C, were calculated for the physiological reaction (CA-asp → DHO) using the formulas:

$$^{15}K_{eq} = {}^{15}(V/K)_{forward}/{}^{15}(V/K)_{reverse} \quad (6)$$

and

$$^{13}K_{eq} = {}^{13}(V/K)_{forward}/{}^{13}(V/K)_{reverse} \quad (7)$$

Using the experimental kinetic and equilibrium isotope effects for hDHOase allowed the kinetic isotope effects for the physiological reaction of CA-asp → DHO to be calculated by rearranging eqs 6 and 7 to $(V/K)_{reverse} = {}^{13}(V/K)_{forward}/{}^{13}K_{eq}$ and $^{15}(V/K)_{reverse} = {}^{15}(V/K)_{forward}/{}^{15}K_{eq}$.

Acid Hydrolysis of CA-asp. CA-asp (17 mg, 100 μM) was placed in a thick-walled 50 mL pear-shaped flask to which was added 13 mL of concentrated HCl and a stir bar. The flask was sealed with a vacuum stopcock using Krytox LVP grease that is inert even when exposed to concentrated acids at high temperature. Krytox was also used in the vacuum stopcock. A two-piece galvanized steel sleeve was fitted around the collar of the flask and held in place with stainless steel wing nuts. Heavy rubber bands or sections of surgical tubing were wrapped around the vacuum stopcock and then the galvanized steel sleeve to hold the pieces together securely. A galvanized steel cup was also fitted to the back of the stopcock which allowed large rubber bands or surgical tubing to be attached and then wrapped around the front of the stopcock, preventing it from ejecting under pressure. The

solution was taken through three freeze−pump−thaw cycles at −130 °C (liquid N_2/pentane) to remove all gases. The flask was placed in a sand bath and heated to 110−115 °C for 7 days behind a blast shield in a laboratory hood. (This methodology proved to be slightly dangerous so a drawing of the reaction vessel and a list of precautions are available as Supporting Information.)

The sample unit was removed from the heat and allowed to cool to room temperature. The unit was attached to a high vacuum distillation line and frozen at −130 °C. CO_2 generated from the decomposition of the amide portion of the molecule was distilled through two −130 °C traps and collected at −196 °C. The $^{13}C/^{12}C$ ratio of the CO_2 was determined by IRMS. These values were used to calculate the secondary kinetic isotope effect of the reverse reaction of DHO → CA-asp catalyzed by DHOase.

Analysis of N_2 from the Amide Portion of CA-asp To Determine the Primary Kinetic Isotope Effect for the Ring Opening of DHO. The residual HCl solution was taken to dryness by rotary evaporation and the residue placed under high vacuum for several hours to ensure all of the HCl had been removed. The residue of NH_4Cl/aspartic acid was dissolved in 100 mL of distilled water and adjusted to pH 6 with 0.5 M KOH. The solution was loaded onto an AG1-X8 column (Cl form, 2.5 × 10 cm) at 1 mL/min. Fraction collection (8 mL/fraction) was started with the loading of the material; the column was then washed with 100 mL of distilled water at 1.0 mL/min. The NH_4Cl was collected from 15 to 130 mL and identified by testing 50 μL aliquots of each fraction with 50 μL of Nessler's reagent in a microwell plate. A positive test was indicated by the appearance of a bright yellow color. The fractions containing NH_4Cl were pooled, rotary evaporated to ≈1 mL, and transferred to a dual compartment sample holder. The second compartment was filled with ≈4 mL of NaOBr. The system was sealed with a stopcock, and the solution was frozen at −78 °C and taken through three freeze−pump−thaw cycles to remove all gases. After the final thaw, the two solutions were mixed slowly, and the liquid was again frozen at −78 °C. The freshly produced N_2 was distilled through two −78 °C traps and one −196 °C trap and then collected on molecular sieves at −196 °C. The N_2 was analyzed by IRMS to give the $^{15}N/^{14}N$ ratio. This ratio was used to calculate the first primary kinetic isotope effect of the ring opening of DHO to CA-asp catalyzed by DHOase.

Analysis of CO_2 from the β-Decarboxylation of Aspartic Acid To Determine the Primary Kinetic Isotope Effect for the Ring Opening of DHO. The aspartic acid portion of the hydrolyzed CA-asp was eluted from the AG1-X8 column with 3 M formic acid between 40 and 60 mL, detected by ninhydrin testing. The fractions containing aspartic acid were pooled and taken to dryness by rotary evaporation and then placed under high vacuum for several hours to ensure that all residual formic acid had been removed.

Aspartic acid samples were dissolved in 4 mL of 50 mM potassium phosphate buffer (pH 7.5) and placed in a 15 mL cylindrical flask equipped with a sidearm stopcock. To this was added 1 mL of 500 mM α-ketoglutarate. The pH of the solution was adjusted to 7.5 with a few drops of 8 M KOH. The flask was sealed with a vacuum stopcock and the sidearm fitted with a septum. The mixture was degassed in vacuo with a series of freeze−pump−thaw cycles. After evacuation, the sample was sparged with dry, CO_2-free, N_2 gas. Aspartate aminotransferase (200 units) and oxaloacetate decarboxylase (150 units) were added via a gastight syringe. The mixture was stirred gently for 48 h at 4 °C. When the decarboxylation was complete, 200 μL of 6 M H_2SO_4 was added via a syringe, and the solution was stirred vigorously for 1 h at room temperature. The sample unit was attached to a high vacuum distillation line and frozen at −78 °C. CO_2 generated from the enzymatic processes was distilled through two −78 °C traps and collected at −196 °C. The $^{13}C/^{12}C$ ratio of the CO_2 was determined by IRMS. These values were used to calculate the second primary kinetic isotope effect of the reverse reaction of DHO → CA-asp catalyzed by DHOase.

RESULTS

Using the internal competition method and isotope ratio mass spectrometry (IRMS) to determine primary and secondary kinetic isotope effects in enzymatic reactions requires that two important conditions be met. First, the atoms of interest in the product or the residual substrate must be converted chemically or enzymatically to a molecule that is easily measured in the IRMS (N_2, CO_2, or H_2), and second, during the conversion no further isotopic fractionation or exchange occurs at these sites. In this study, these requirements were met by acid hydrolysis of the product CA-asp and then oxidation or enzymatic decomposition of those hydrolysis products (Scheme 2). The hydrolysis using concentrated HCl allowed the direct production of CO_2 from C4 of the CA-asp molecule that was purified on a high vacuum line and analyzed by IRMS to determine the secondary kinetic isotope effect of the DHO → CA-asp reaction. The HCl was removed in vacuo leaving NH_4Cl and aspartic acid. These were easily separated by column chromatography, and the NH_3 originating from N3 of CA-asp was steam distilled, oxidized with NaOBr to N_2, and analyzed by IRMS to determine the first of the primary kinetic isotope effects for the DHOase reaction. Lastly, the residual aspartic acid from the HCl hydrolysis of CA-asp was converted to pyruvate and CO_2 using glutamic−oxaloacetic transaminase and oxaloacetate decarboxylase. The CO_2 produced contained C2 from CA-asp and was analyzed by IRMS to determine the second primary kinetic isotope effect for the system.

Kinetic Isotope Effects. The values for the kinetic isotope effects for the conversion of DHO → CA-asp by hDHOase and BcDHOase are shown in Table 1. The reactions were run from 25 to 45 °C for hamster and 37−60 °C for *B. caldolyticus.* The differences in kinetic isotope effects due to temperature change are nonexistent for hDHOase and show a very moderate difference in the secondary kinetic isotope effect for BcDHOase even though both systems were run at suboptimal temperatures. The average kinetic isotope effects across the temperature ranges for the two enzymes are shown in Table 2. These data also illustrate that there is no statistical difference in the kinetic isotope effects for the mechanisms catalyzed by these type 1 DHOases. The secondary kinetic isotope effects for hDHOase and BcDHOase are slightly normal (>1.0000). However, the errors are large enough that the isotope effects are not significantly different. The primary kinetic isotope effects for both enzymes are nearly identical.

Table 1: Isotope Effect Results for Conversion of DHO to CA-asp Catalyzed by DHOases from Hamster and *B. caldolyticus*

DHOase	temp (°C)	IE/gas	IE value[a]
hamster	25	secondary/CO_2	1.0006 ± 0.0024
hamster	25	primary/N_2	1.0112 ± 0.0005
hamster	25	primary/CO_2	1.0121 ± 0.0003
hamster	37	secondary/CO_2	0.9993 ± 0.0056
hamster	37	primary/N_2	1.0110 ± 0.0003
hamster	37	primary/CO_2	1.0092 ± 0.0032
hamster	45	secondary/CO_2	1.0020 ± 0.0028[b]
hamster	45	primary/N_2	1.0098 ± 0.0006
hamster	45	primary/CO_2	1.0107 ± 0.0003
B. caldolyticus	37	secondary/CO_2	0.9992 ± 0.0020
B. caldolyticus	37	primary/N_2	1.0131 ± 0.0010[c]
B. caldolyticus	37	primary/CO_2	1.0109 ± 0.0004
B. caldolyticus	50	secondary/CO_2	1.0054 ± 0.0028[b]
B. caldolyticus	50	primary/N_2	1.0120 ± 0.0006
B. caldolyticus	50	primary/CO_2	1.0076 ± 0.0019
B. caldolyticus	60	secondary/CO_2	1.0039 ± 0.0020
B. caldolyticus	60	primary/N_2	1.0123 ± 0.0010[c]
B. caldolyticus	60	primary/CO_2	1.0089 ± 0.0015

[a] Each value was determined from two samples except for those indicated. [b] Estimated error using all secondary kinetic isotope effect data. [c] Estimated error using all primary kinetic isotope effect data from N_2 studies.

Table 2: Average Kinetic Isotope Effects for Reaction of DHO to CA-asp Catalyzed by DHOases from Hamster and *B. caldolyticus*

DHOase	IE/gas	IE value
hamster	secondary/CO_2	1.0006 ± 0.0036
hamster	primary/N_2	1.0107 ± 0.0006
hamster	primary/CO_2	1.0107 ± 0.0012
B. caldolyticus	secondary/CO_2	1.0028 ± 0.0026
B. caldolyticus	primary/N_2	1.0125 ± 0.0009
B. caldolyticus	primary/CO_2	1.0091 ± 0.0014

Table 3: Equilibrium Isotope Effects for Reaction of DHO to CA-asp Catalyzed by DHOase from Hamster

	temp (°C)	K_{eq}IE/gas	K_{eq}IE
hamster	25	secondary/CO_2	1.0028 ± 0.0002
hamster	25	primary/N_2	1.0053 ± 0.0003
hamster	25	primary/CO_2	1.0027 ± 0.0003

Equilibrium Isotope Effect for the Interconversion of DHO and CA-asp. To determine the equilibrium isotope effect, the reaction was allowed to proceed approximately 10 times the time required to reach equilibrium, the products were separated, and isotopic analysis was used to determine the mass ratios (Materials and Methods). Table 3 shows the equilibrium isotope effects for the interconversion of DHO and CA-asp by hDHOase.

Calculated Kinetic Isotope Effects for CA-asp → DHO Catalyzed by hDHOase. The equilibrium isotope effect is the ratio of $^{13}(V/K)$ or $^{15}(V/K)$ for the forward and the reverse reactions (Materials and Methods). Thus it is possible to experimentally determine the kinetic isotope effect for the cyclization of CA-asp → DHO by hDHOase using the experimental equilibrium isotope effects and kinetic isotope effects (Table 4).

Table 4: Calculation of Kinetic Isotope Effects for Cyclization of CA-asp to DHO Using Equilibrium and Kinetic Isotope Effects

DHOase	temp (°C)	KIE/gas	calculated KIE[a]
hamster	25	secondary/CO_2	0.9978 ± 0.0036
hamster	25	primary/N_2	1.0054 ± 0.0006
hamster	25	primary/CO_2	1.0079 ± 0.0012

[a] The errors are assumed to be identical to those of the forward reaction.

DISCUSSION

Primary Isotope Effects. Kinetic isotope effects reflect changes in the bond orders of the substrate between ground state and transition state. Kinetic isotope effects, when measured by internal competition, are effects on *V*/*K* and as such take into account any step of the reaction up to and including the first irreversible step (*18*). Primary kinetic isotope effects involve bond making or breaking to the isotopic atom and are almost always normal. A primary kinetic isotope effect of unity indicates that the rate-limiting step of the system is not the chemistry but more likely conformational changes, binding, or release of the product, any of which can influence the overall rate of an enzyme-catalyzed reaction (*19*, *20*). However, since the overall rate of an enzymatically catalyzed reaction is defined as the reciprocal of the sum of the reciprocal net rate constants, even if the primary kinetic isotope effect is greater than unity, it is not necessarily true that the chemistry is fully rate-limiting in the system. The positive value indicates only that the chemistry of the reaction is at least *partially* rate-limiting as there is a possibility that a nonchemical step may be of nearly the same rate and may also play a role in overall rate limitation of the reaction (*18*). If the same reaction is done *nonenzymatically* and the kinetic isotope effect values are equivalent to the enzymatic values (assuming the mechanisms are identical), then it can be reasonably assumed that chemistry is predominantly rate-limiting. Unfortunately, the kinetic isotope effect values for the nonenzymatic conversion of DHO → CA-asp have not been determined, and thus it cannot be assumed that some other process does not have at least a limited role in the overall rate of the reaction.

The average carbon and nitrogen primary kinetic isotope effects for the reaction of DHO → CA-asp catalyzed by the two type 1 DHOases in this study are statistically the same at approximately 1.1%. In comparison, the ^{15}N kinetic isotope effect for the enzymatic hydrolysis of *N*-acetyl-L-tryptophanamide by chymotrypsin is nearly identical at 1.010 ± 0.001 (*21*) while the papain-catalyzed hydrolysis of *N*-benzoyl-L-arginamide is nearly double at 1.021 ± 0.001 (*22*). All three values are well short of theoretical maximum kinetic isotope effect for C−N bond breaking which is calculated to be 1.044 (*23*).

The primary kinetic isotope effects for the conversion of DHO → CA-asp by either DHOase show no significant change over the temperature ranges studied. This indicates that the rates of binding, conformational changes, and product release remain unaffected by moderate changes in temperature and remain faster than the chemistry in the temperature range studied. In the case of thermophilic enzymes (such as *B. caldolyticus*) at lower temperatures the binding or conformational changes in the enzyme may slow to the point where they can become the rate-limiting step for a reaction, and thus any normal kinetic isotope effect of the chemical step could be "washed out", giving a value of unity. This lack of change in kinetic isotope effect from 25 to 45 °C (hamster) and 37−60 °C (*B. caldolyticus*) suggests that for DHOase the chemistry may be largely rate limiting.

Scheme 3

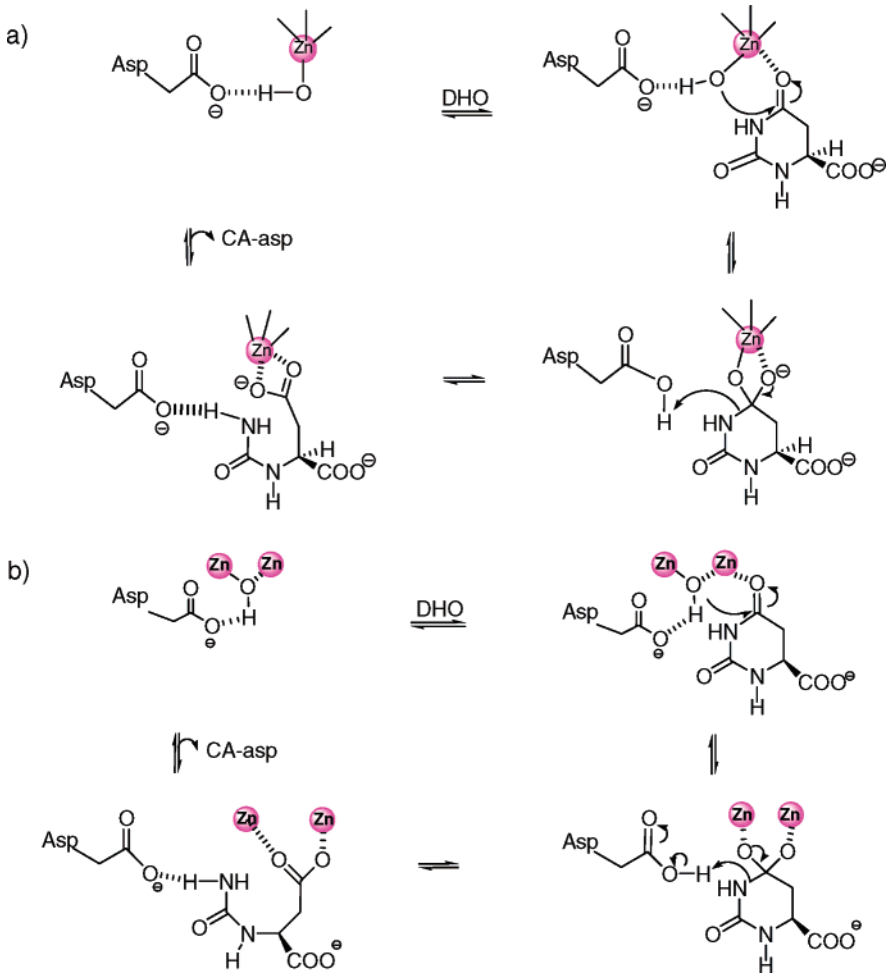

The crystallographic structure of the type I DHOase from *A. aeolicus* shows a single zinc atom bound by two histidine residues, an aspartate, and a hydroxide ion or water molecule (*14*; Scheme 3a). A similar arrangement with a single zinc coordinated by three histidines was proposed for the DHOase domain of CAD from hamster (*16*). When DHO enters the active site, the oxygen (O4) of the carbonyl group may interact with the zinc ion polarizing the C−O bond and increasing the electrophilicity of the carbonyl carbon (C4). The coordinated H_2O/hydroxide acts as a nucleophile and attacks the carbonyl group carbon (C4). As this attack occurs, the proton on the H_2O/hydroxide is simultaneously transferred to a second aspartate (not ligated to Zn) and a tetrahedral intermediate is formed coordinated to the zinc. The same proton is then abstracted by N3 from the aspartate, the tetrahedral intermediate collapses, and C−N bond scission occurs. Similar mechanisms for other members of the amidohydrolase family have been proposed recently (*24*, *25*). For the type II DHOase from *E. coli*, a similar mechanism of catalysis was also proposed (*7*, *9*, *11*, *26*; Scheme 3b). The two active site Zn ions are bridged by a hydroxide group from a water molecule, and the conserved aspartate interacts with the α Zn ion.

Secondary Isotope Effects. In secondary kinetic isotope effects, the atom of interest is bonded to one of the atoms involved in bond scission. Isotope effects are due mainly to differences in stretching modes, but when no bond fission at the isotopic atom is occurring, changes in the other vibrational modes (bending and torsional) become more important and are sensitive to any change in bond order, or bond "stiffness" (*27*). A normal secondary KIE means the bond order at the atom is becoming smaller; it is bonded less stiffly in the transition state. An inverse kinetic isotope effect (<1.000) shows that at the transition state the atom is more stiffly bonded.

The secondary kinetic isotope effects in the present study are unity or very slightly normal, indicating that there is only a very slight decrease in the stiffness of bonding at the C2 carbon of DHO as it ring opens to CA-asp. The secondary ^{13}C equilibrium isotope effect is well determined and is 0.28% normal due to small overall changes in torsional and bending modes between DHO and CA-asp shown in Scheme 4. The small size of the kinetic secondary isotope effects and their errors do not permit any definitive statements about transition state structure except that it is intermediate in structure between substrate and product.

Equilibrium Isotope Effects and Calculated Kinetic Isotope Effects for the Reaction Catalyzed by hDHOase. Equilibrium isotope effects result from the differences in the stiffness of bonding of the substituted atom in the substrate and product (*28*). The equilibrium isotope effects in Table 3 demonstrate that ^{13}C and ^{15}N are more stiffly bonded at C4 and N3 in DHO than in CA-asp.

Having the kinetic and equilibrium isotope effects for hDHOase allowed the kinetic isotope effects for the physiological reaction of CA-asp → DHO to be calculated by

Scheme 4: Interpretation of Secondary Isotope Effect Studies[a]

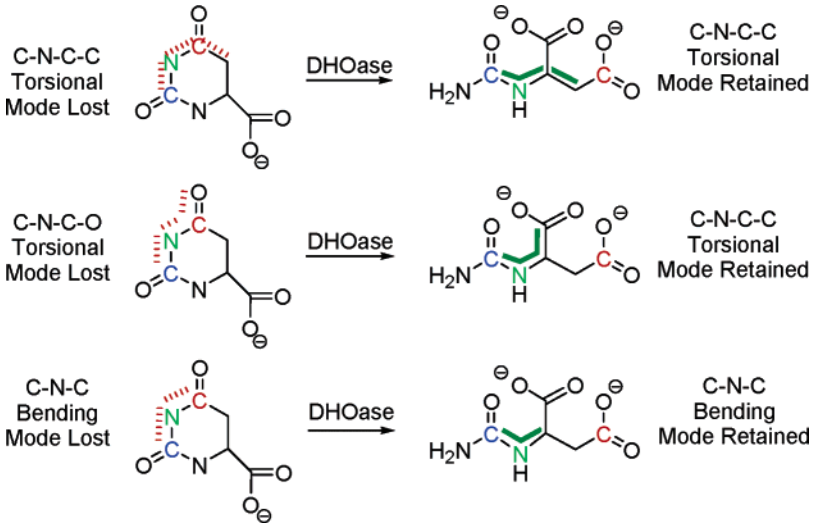

[a] Isotope effects are due mainly to differences in bond stretching modes. However, when no bond fission at the isotopic atom is occurring, changes in the other vibrational modes (bending and torsional modes) become more important and are sensitive to any change in bond order, or bond "stiffness". In these experiments the small secondary isotope effects indicate that the loss of the torsional and bending modes on ring opening of DHO does not affect the overall bond stiffness to a great extent since, while some modes are lost, others are retained in CA-asp.

rearranging eqs 6 and 7 to $(V/K)_{reverse} = {}^{13}(V/K)_{forward}/{}^{13}K_{eq}$ and ${}^{15}(V/K)_{reverse} = {}^{15}(V/K)_{forward}/{}^{15}K_{eq}$ (Table 4). In this case, the secondary kinetic isotope effect is shown to be slightly inverse although the error is probably too high to make any definitive statement on the meaning of the value. The ^{13}C and ^{15}N primary kinetic isotope effects of 0.79% and 0.54% are normal.

The putative mechanism of the reaction (Scheme 3a) involves two steps: the formation and breakdown of a tetrahedral intermediate. The approximately 1% primary isotope effect suggests that the step in which C−N cleavage or bond formation occurs is a major rate-limiting step (Scheme 3). The other step, attack of the hydroxide on C-4 of DHO, or its elimination in the reverse direction, should produce a primary isotope effect at C4, but not at N-3. The near equality of the ^{13}C isotope effect at C-4 and the ^{15}N at N-3 suggests that this step is not a major rate-limiting one, as otherwise the primary isotope effect at C-4 should be larger than the ^{15}N one. This conclusion makes sense, since attack by an OH on a Zn-polarized carbonyl is expected to be a facile reaction, while attack of an amide, even with general base assistance by aspartate, on a carbonyl carbon is much more difficult, although polarization by a Zn ion will make the carbonyl carbon at least somewhat electrophilic.

SUMMARY

The data for the reaction studied (DHO → CA-asp) show normal primary kinetic isotope effects of moderate size and suggest that the chemistry for the reactions catalyzed by the type I DHOases from hamster and *B. caldolyticus* are at least partially rate-limiting. The slight, but still normal, secondary kinetic isotope effects indicate that the effect is due to the loss of some bonding stiffness at the C atom upon ring opening of DHO. The equilibrium isotope effects indicate that the heavier isotopes tend to accumulate in DHO where they are more stiffly bound. The calculated kinetic isotope effects for the physiological reaction of CA-asp → DHO are slightly smaller than those of the reverse direction but are still normal, signifying that the chemistry is still at least partially rate-limiting in the forward direction.

SUPPORTING INFORMATION AVAILABLE

Further description of the details, materials, and dangers of the acid hydrolysis of DHO and CA-asp is available free of charge via the Internet at http://pubs.acs.org.

REFERENCES

1. Christopherson, R. I., and Jones, M. E. (1980) The overall synthesis of L-5,6-dihydroorotate by multi-enzymatic protein *pyr1-3* from hamster cells, *J. Biol. Chem. 255*, 11381−11395.
2. Huang, D. T. C., Thomas, M. A. W., and Christopherson, R. I. (1999) Divalent metal derivatives of the hamster dihydroorotase domain, *Biochemistry 38*, 9964−9970.
3. Christopherson R. I., Schmalzl, K. J., Szabados, E., Goodridge R. J., Harsanyi, M. C., Sant, M. E., Algar, E. M., Anderson, J. E., and Armstrong, A. (1989) Mercaptan and dicarboxylate inhibitors of hamster dihydroorotase, *Biochemistry 28*, 463−470.
4. Christopherson, R. I., Lyons, S. D., and Wilson, P. K. (2002) Inhibitors of de novo nucleotide biosynthesis as drugs, *Acc. Chem. Res. 35*, 961−971.
5. Levenson, C. H., and Meyer, R. B., Jr. (1984) Design and synthesis of tetrahedral intermediate analogues as potential dihydroorotase inhibitors, *J. Med. Chem. 27*, 228−232.
6. Adams, J. L., Meek, T. D., Mong, S. M., Johnson, R. K., and Metcalf, B. W. (1988) *cis*-4-Carboxy-6-(mercaptomethyl)-3,4,5,6-tetrahydropyrimidin-2(1*H*)-one, a potent inhibitor of mammalian dihydroorotase, *J. Med. Chem. 31*, 1355−1359.
7. Thoden, J. B., Phillips, G. N., Jr., Neal, T. M., Raushel, F. M., and Holden, H. M. (2001) Molecular structure of dihydroorotase: A paradigm for catalysis through the use of a binuclear metal center, *Biochemistry 40*, 6989−6997.
8. Purcarea, C., Martin, P., Vickery, J. F., Guy, H. I. Edwards, B. F. P., and Evans, D. R. (2002) Cloning expression and preliminary X-ray analysis of the dihyroorotase from the hyperthermophilic eubacterium *Aquifex aeolicus*, *Acta Crystallogr., Sect. D: Biol. Crystallogr. 5*, 154−156.
9. Maher, M. J., Huang, D. T. C., Guss, J. M., Collyer, C. A., and Christopherson, R. I. (2003) Crystallization of hamster dihydroorotase: Involvement of a disulfide-linked tetrameric form, *Acta Crystallogr., Sect. D: Biol. Crystallogr. 59*, 381−384.
10. Holm, L., and Sander, C. (1997) An evolutionary treasure: unification of a broad set of amidohydrolases related to urease, *Proteins: Struct., Funct., Genet. 28*, 72−82.

11. Seibert, C. M., and Raushel, F. M. (2005) Structural and catalytic diversity within the amidohydrolase superfamily, *Biochemistry 44*, 6383−6391.
12. Wilson, D. K., Rudolf, F. B., and Quiocho, F. A. (1991) Atomic structure of adenosine deaminase complexed with a transition-state analog: Understanding catalysis and immunodeficiency mutations, *Science 252*, 1278−1284.
13. Fields, C., Brichta, D., Sheperdson, M., Farinha., and O'Donovan, G. (1999) Pyrimidine metabolism in plants, *Paths Pyrimidines 7*, 49−62.
14. Martin, P. D., Purcarea, C., Zhang, P., Vaishnav, A., Sadecki, S., Guy-Evans, H. I., Evans, D. R., and Edwards, B. F. P. (2005) The crystal structure of a novel, latent dihydroorotase from *Aquifex aeolicus* at 1.7 Å resolution, *J. Mol. Biol. 348*, 535−547.
15. Lee, M., Chan, C. W., Guss, J. M., Christopherson, R. I., and Maher, M. J. (2005) Dihydroorotase from *Escherichia coli*: Loop movement and cooperativity between subunits, *J. Mol. Biol. 348*, 523−533.
16. Williams, N. K., Peide, Y., Seymour, K. K., Ralston, G. B., and Christopherson, R. I. (1993) Expression of catalytically active hamster dihydroorotase domain in *Escherichia coli*: Purification and characterization, *Protein Eng. 6*, 333−340.
17. Northrup, D. B. (1977) *Isotope Effects on Enzyme-Catalyzed Reactions* (Cleland, W. W., O'Leary, M. H., and Northrup, D. B., Eds.) pp 122−152, University Park Press, Baltimore, MD.
18. Cleland, W. W. (1975) What limits the rate of an enzyme-catalyzed reaction, *Acc. Chem. Res. 8*, 145−151.
19. Northrup, D. B. (1975) Steady-state analysis of kinetic isotope effects in enzymic reactions, *Biochemistry 14*, 2644−2651.
20. Northrup, D. B. (1981) The expression of isotope effects on enzyme-catalyzed reactions, *Annu. Rev. Biochem. 50*, 103−131.
21. O'Leary, M. H., and Kluetz, M. D. (1970) Identification of the rate-limiting step in the chymotrypsin-catalyzed hydrolysis of *N*-acetyl-L-tryptophanamide, *J. Am. Chem. Soc. 92*, 6089−6090.
22. O'Leary, M. H., Urberg, M., and Young, A. P. (1974) Nitrogen isotope effects on the papain-catalyzed hydrolysis of *N*-benzoyl-L-argininamide, *Biochemistry 13*, 2077−2081.
23. Huskey, W. P. (1991) in *Enzyme Mechanisms from Isotope Effects* (Cook, P. F., Ed.) pp 37−72, CRC Press, Boca Raton, FL.
24. Aubert, S. D., Li, Y., and Raushel, F. M. (2004) Mechanism for the hydrolysis of organophosphates by the bacterial phosphotriesterase, *Biochemistry 43*, 5707−5715.
25. Thoden, J. B., Marti-Arbona, R., Raushel, F. M., and Holden, H. M. (2003) High-resolution X-ray structure of isoaspartyl dipeptidase from *Escherichia coli*, *Biochemistry 42*, 4874−4882.
26. Porter, T. N., Li, Y., and Raushel, F. M. (2004) Mechanism of the dihyroorotase reaction, *Biochemistry 43*, 16285−16292.
27. Bigeleisen, J., and Mayer, M. G. (1947) Calculation of equilibrium constants for isotope exchange reactions, *J. Chem. Phys. 15*, 261−267.
28. Cleland, W. W. (1982) Use of isotope effects to elucidate enzyme mechanisms, *CRC Crit. Rev. Biochem. 13*, 387−428.

BI0604025